

Dynamical effects of breaking rotational symmetry in counter-rotating Stuart-Landau oscillatorsNirmal Punetha,¹ Vaibhav Varshney,² Samir Sahoo,³ Garima Saxena,⁴ Awadhesh Prasad,² and Ram Ramaswamy³¹*Max Planck Institute for the Physics of Complex Systems, Nöthnitzer Straße 38, D-01187 Dresden, Germany*²*Department of Physics and Astrophysics, University of Delhi, Delhi 110007, India*³*School of Physical Sciences, Jawaharlal Nehru University, Delhi 110067, India*⁴*Department of Physics, Sri Venkateswara College, University of Delhi, Delhi 110021, India*

(Received 8 July 2018; published 17 August 2018)

Stuart-Landau oscillators can be coupled so as to either preserve or destroy the rotational symmetry that the uncoupled system possesses. We examine some of the simplest cases of such couplings for a system of two nonidentical oscillators. When the coupling breaks the rotational invariance, there is a qualitative difference between oscillators wherein the phase velocity has the same sign (termed co-rotation) or opposite signs (termed counter-rotation). In the regime of oscillation death the relative sense of the phase rotations plays a major role. In particular, when rotational invariance is broken, counter-rotation or phase velocities of opposite signs appear to destabilize existing fixed points, thereby preserving and possibly extending the range of oscillatory behavior. The dynamical “frustration” induced by counter-rotations can thus suppress oscillation quenching when coupling breaks the symmetry.

DOI: [10.1103/PhysRevE.98.022212](https://doi.org/10.1103/PhysRevE.98.022212)**I. INTRODUCTION**

The collective behavior of ensembles of interacting oscillators has been of considerable interest in a number of disciplines in both the natural as well as the social sciences [1–4]. The nature of the collective behavior depends to a large extent upon the dynamical properties of the individual units as well as on the nature of the coupling [5]. It is known, for instance, that different types of internal dynamics give rise to different scenarios of synchronization [2,3,6]. Furthermore, different types of coupling interactions lead to interesting spatio-temporal behavior such as traveling wave solutions, chimeric states, or glassy dynamics [7–9]. The coupling can also destroy oscillations; this is the phenomenon of oscillation quenching [10–15], namely, the *suppression* of oscillations as a consequence of the coupling. When this occurs, oscillators appear to drag each other towards a fixed point and reach an equilibrium. This may happen when the coupling between the oscillators stabilizes one of the previously unstable fixed points, termed amplitude death (AD). Alternatively, a new set of stable fixed points may be created, and this is termed oscillation death (OD) [14].

A number of studies of coupled oscillator systems have focused on the Stuart-Landau (SL) oscillator since it provides a universal model for the dynamics in the vicinity of a supercritical Hopf bifurcation [16]. The equation of motion for this system can be written in the form

$$\dot{z} = (1 + i\omega - |z|^2)z, \quad (1)$$

where z is a complex variable and ω is the oscillation frequency. Under the transformation $z \rightarrow ze^{i\Omega t}$, the form of the equation remains unchanged, albeit with frequency $\omega \rightarrow \omega + \Omega$.

This rotational invariance may be preserved or destroyed when two or more such oscillators are coupled, and in the present work, our interest is in examining the dynamical

consequences of breaking rotational symmetry. We therefore study the manner in which the relative phase velocity affects the collective dynamics in coupled SL systems. For two coupled oscillators, the phase velocities can either have the same sign, in which case these are termed co-rotating, or can have opposite signs, in which case they are counter-rotating [17]. When rotational invariance is preserved, a suitable choice of Ω can remove the distinction between co- and counter-rotation. When rotational invariance is broken, though, the cases of co- and counter-rotation act differently.

A number of commonly studied chaotic oscillator systems possess discrete symmetries, and the effect of couplings that keep or break these symmetries has also been studied in a number of papers [12,18,19]. It is known that for a network of nonlocally coupled identical SL oscillators with symmetry broken coupling shows various dynamical states such as amplitude chimeras, amplitude cluster, frequency chimera, frequency cluster states [18], and stable and transient multiclustered patterns [19], as the coupling range is increased a novel pattern termed chimera death was observed by Zakharova *et al.* [20]. Time-delayed coupling also breaks the rotational symmetry, and similar phenomena of amplitude death are observed for two or more SL oscillators coupled via time delayed coupling [12]. Clustered chimera states exist in a ring of such oscillators [21], and the lifetime of the chimeras can be significantly enhanced by coupling delay [22]. It is interesting to note that competing effects between attractive and repulsive couplings induce spontaneous symmetry breaking in a homogenous system of coupled oscillators [23].

As we see in the following section wherein we describe the model of coupled SL oscillators and discuss the nature of their interaction, linear forms of the coupling will preserve the rotational symmetry. Nonlinear couplings often break invariance, and we study some simple cases. We recover the instance of coupling between dissimilar variables (termed

conjugate coupling in earlier work [14]) as a special case and present analytical and numerical results for the cases of co- and counter-rotation in Sec. II for the rotational symmetry-preserving as well as rotational symmetry-breaking cases. This is followed by a discussion and summary in Sec. III.

II. COUPLED OSCILLATORS

Consider a system of two coupled SL oscillators

$$\dot{z}_k = (1 + i\omega_k - |z_k|^2)z_k + \varepsilon g_k(z_k, z_j), \quad (2)$$

where $j, k = 1, 2$, and $j \neq k$. We take the frequencies ω_k to be distinct, ε is the coupling strength, and g_k are coupling functions. It is convenient to consider the system in coordinates x_k, y_k with $z_k = x_k + iy_k$, in which the equations of motion read

$$\begin{aligned} \dot{x}_k &= [1 - (x_k^2 + y_k^2)]x_k - \omega_k y_k + \varepsilon g_{kr}, \\ \dot{y}_k &= [1 - (x_k^2 + y_k^2)]y_k + \omega_k x_k + \varepsilon g_{ki}, \end{aligned} \quad (3)$$

with $k = 1, 2$, and g_{kr} and g_{ki} denote the real and imaginary parts of the coupling functions, g_k .

In the absence of coupling, namely for $\varepsilon = 0$, the relative signs of ω_1 and ω_2 are inconsequential: they can be made identical or different by transforming to a common rotating frame $z_k \rightarrow z_k e^{i\Omega t}$ and by suitably choosing Ω , the sign of effective frequency ($\omega_k + \Omega$) can be made positive or negative. Clearly, rotational symmetry is preserved if under this transformation the coupling function also transforms in the same way, namely, $g_k \rightarrow g_k e^{i\Omega t}$.

Below we discuss both types of coupling and contrast the dynamics that results when the phase velocities have similar or opposite signs, namely the cases of co- and counter-rotation.

A. Symmetry-preserving case

In this section we consider two different coupling schemes which preserve rotational symmetry in the coupled SL system. The most commonly considered case is of linear coupling between the oscillators:

$$\begin{aligned} \dot{z}_1 &= (1 + i\omega_1 - |z_1|^2)z_1 + \varepsilon(z_2 - z_1), \\ \dot{z}_2 &= (1 + i\omega_2 - |z_2|^2)z_2 + \varepsilon(z_1 - z_2). \end{aligned} \quad (4)$$

Separating into real and imaginary parts, one can rewrite the above equations as

$$\begin{aligned} \dot{x}_i &= [1 - (x_i^2 + y_i^2)]x_i - \omega_i y_i + \varepsilon(x_j - x_i), \\ \dot{y}_i &= [1 - (x_i^2 + y_i^2)]y_i + \omega_i x_i + \varepsilon(y_j - y_i) \end{aligned} \quad (5)$$

with $i, j = 1, 2$, and $j \neq i$.

The origin $(x_1^*, y_1^*, x_2^*, y_2^*) = (0, 0, 0, 0) \equiv z^c$ in the coupled system is an equilibrium. Around this fixed point, the linearized dynamics is given by $\delta\dot{z} = \mathbf{J}|_{z^c=0}\delta z$, where $\delta z = (\delta x_1, \delta y_1, \delta x_2, \delta y_2)^T$ and the Jacobian matrix is

$$\mathbf{J}|_{z^c} = \begin{pmatrix} 1 - \varepsilon & -\omega_1 & \varepsilon & 0 \\ \omega_1 & 1 - \varepsilon & 0 & \varepsilon \\ \varepsilon & 0 & 1 - \varepsilon & -\omega_2 \\ 0 & \varepsilon & \omega_2 & 1 - \varepsilon \end{pmatrix}. \quad (6)$$

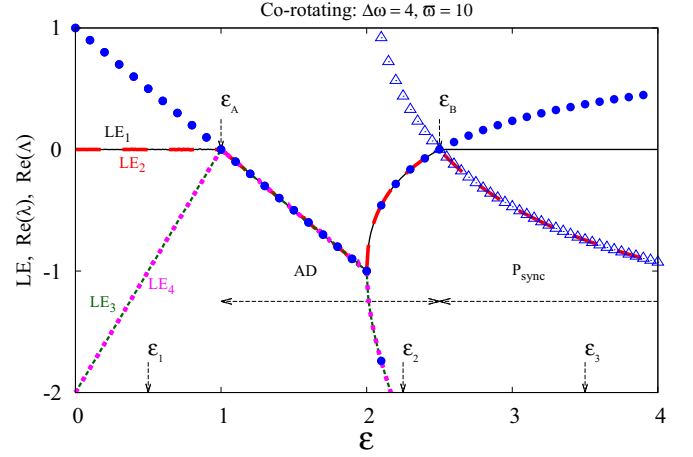


FIG. 1. Lyapunov exponents of the system coupled through similar variables [Eq. (5)] are plotted as function of coupling strength ε with lines (solid, long-dashed, short-dashed, and dotted lines for $LE_{1,2,3,4}$, respectively), along with the real part of the eigenvalues λ [filled circle, Eq. (7)] and Λ [open triangles, Eq. (13)].

The stability of the origin is determined by the eigenvalues λ of \mathbf{J} , which can easily be shown to be

$$\lambda = 1 - \varepsilon \mp \sqrt{\varepsilon^2 - \frac{\Delta\omega^2}{4}} \mp i\bar{\omega}, \quad (7)$$

where mismatch $\Delta\omega = \omega_1 - \omega_2$ and average frequency $\bar{\omega} = (\omega_1 + \omega_2)/2$. The real and imaginary parts of the eigenvalues are

$$\begin{aligned} \text{Re}(\lambda) &= (1 - \varepsilon), \text{ if } \varepsilon \leq \frac{\Delta\omega}{2} \\ &= (1 - \varepsilon) \mp \sqrt{\varepsilon^2 - \frac{\Delta\omega^2}{4}}, \text{ if } \varepsilon > \frac{\Delta\omega}{2} \end{aligned} \quad (8)$$

and

$$\begin{aligned} \text{Im}(\lambda) &= \mp \sqrt{\left|\varepsilon^2 - \frac{\Delta\omega^2}{4}\right|} \mp \bar{\omega}, \text{ if } \varepsilon \leq \frac{\Delta\omega}{2} \\ &= \mp \bar{\omega}, \text{ if } \varepsilon > \frac{\Delta\omega}{2}. \end{aligned} \quad (9)$$

The stability is determined by the largest real part of the eigenvalues, and this turns out to be independent of $\bar{\omega}$: thus for both co- and counter-rotations, the regions of negative $\text{Re}(\lambda)$ are unaltered, and the parameter windows for which AD is observed in the system are unchanged. From Eq. (8) it can be seen that the critical values of ε that bound the region of AD are $\varepsilon_A = 1$, and $\varepsilon_B = \frac{1}{2}(1 + \Delta\omega^2/4)$, as marked in Fig. 1.

We examine the system by transforming Eq. (5) to polar coordinates, taking $\theta_i = \arctan(y_i/x_i)$ and $r_i = \sqrt{x_i^2 + y_i^2}$, $i = 1, 2$. The dynamics is governed by

$$\begin{aligned} \dot{r} &= r(1 - \varepsilon - r^2) + \varepsilon r \cos \phi, \\ \dot{\phi} &= \Delta\omega - 2\varepsilon \sin \phi, \end{aligned} \quad (10)$$

where $r_1 = r_2 = r$, $\phi = (\theta_2 - \theta_1)$, and $\Delta\omega = (\omega_2 - \omega_1)$. Stationary solutions for the above equation,

$$r^{*2} = 1 - \varepsilon \pm \sqrt{\varepsilon^2 - \left(\frac{\Delta\omega}{2}\right)^2},$$

$$\phi^* = \arcsin\left(\frac{\Delta\omega}{2\varepsilon}\right) \quad (11)$$

will exist for $\varepsilon \geq \Delta\omega/2$. Note that the individual frequencies $\dot{\theta}_{1,2}$ in this state are given by $\dot{\theta}_{1,2} = \omega_{1,2} \pm \Delta\omega/2$, i.e., $\dot{\theta}_{1,2} = \bar{\omega}$, implying that the oscillators are moving with the same collective frequency $\bar{\omega}$. Hence for co-rotating oscillators (when $\bar{\omega} \neq 0$), these solutions correspond to the oscillations with a constant amplitude and a constant phase difference, namely, the phase-locked or synchronized motion with frequency $\bar{\omega}$. These oscillations are suppressed in the counter-rotating system since the frequency is $\bar{\omega} = 0$.

The stability is governed by the eigenvalues of the Jacobian matrix [obtained from Eq. (10)]:

$$\mathbf{H} = \begin{pmatrix} 1 - \varepsilon - 3r^{*2} + \varepsilon \cos \phi^* & -\varepsilon r^* \sin \phi^* \\ 0 & -2\varepsilon \cos \phi^* \end{pmatrix}. \quad (12)$$

Since \mathbf{H} is upper triangular, the eigenvalues $\Lambda_{1,2}$ are given by the diagonal elements, and using Eq. (11) one gets

$$\Lambda_1 = -2(1 - \varepsilon) \mp 2\sqrt{\varepsilon^2 - \Delta\omega^2/4} = -2(1 - \varepsilon) - 2\varepsilon C,$$

$$\Lambda_2 = \mp 2\sqrt{\varepsilon^2 - \Delta\omega^2/4} = -2\varepsilon C, \quad (13)$$

where $C = \cos \phi^* = \pm(1 - \Delta\omega^2/4\varepsilon^2)^{1/2}$. There are two branches of eigenvalues corresponding to the positive and negative values of the quantity C . When $C < 0$, Λ_2 is always positive, indicating that the solution is always unstable. However, when C is positive, the solutions are stable when

$$\varepsilon > \frac{1}{2}(1 + \Delta\omega^2/4), \quad (14)$$

and the resulting dynamics are synchronized oscillatory motion for co-rotating oscillators.

Lyapunov exponents (LEs) of the coupled system Eq. (5) are shown in Fig. 1 along with the real parts of the eigenvalues, namely, Eqs. (8) and (13) for the case of co-rotating oscillators, namely, $\omega_1 = 12$ and $\omega_2 = 8$. These quantities are same for counter-rotating oscillators with equal amount of mismatch $\Delta\omega = 4$, $\bar{\omega} = 0$. In the coupling interval $\varepsilon_A = 1 \leq \varepsilon \leq \varepsilon_B = \frac{1}{2}(1 + \Delta\omega^2/4)$ the origin is stable since $\text{Re}(\lambda) < 0$ (shown by blue circles). Furthermore, the solutions described in Eq. (11) stabilize at $\varepsilon = \frac{1}{2}(1 + \Delta\omega^2/4) = 2.5$ when $\text{Re}(\Lambda)$ (shown by triangles) is less than zero. These correspond to phase-locked periodic solutions (P_{sync}) with frequency $\bar{\omega}$ in the co-rotating case whereas nonoscillatory solutions ($\bar{\omega} = 0$) for the counter-rotating case.

This analysis can be directly verified through simulations. Trajectories in phase space and the corresponding time series are plotted in Fig. 2 for the co-rotating case at select values of ε (marked by arrows in Fig. 1). For small ε , in Fig. 2(a), systems show incoherent oscillatory behavior. For $1 < \varepsilon < 2.5$ the origin is stable and one has amplitude death, so in Fig. 2(b) the trajectories eventually go to the origin. Finally, in Fig. 2(c), one has phase-locked behavior.

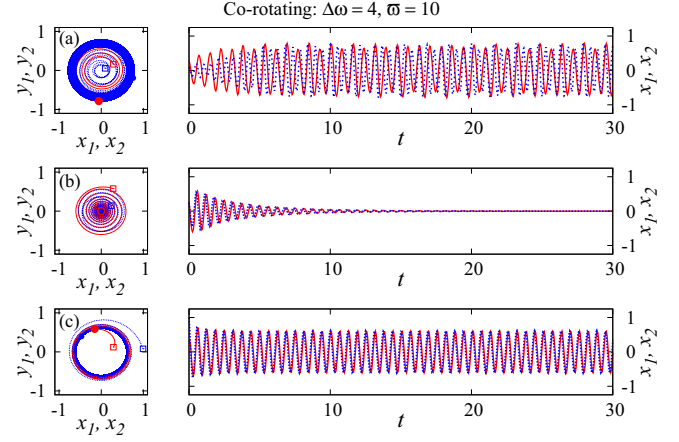


FIG. 2. For similar-variable coupling and co-rotating oscillators [Eq. (5)], shown in left panel is the behavior of the system in phase space (x_i, y_i plane) at different coupling values. Trajectories of two oscillators are shown by solid-red and dotted-blue lines, respectively. The starting point of the two trajectories is shown by open boxes, and the final states are shown by filled circles. Corresponding time series of variables $x_{1,2}$ are plotted on the right panel using solid-red and dotted-blue lines. Panels (a)–(c), respectively, correspond to the behaviors at different coupling values $\varepsilon = 0.5, 2.25, 3.5$, as marked in Fig. 1.

Note that coupling the oscillators via

$$\dot{z}_1 = (1 + i\omega_1 - |z_1|^2)z_1 + \varepsilon \frac{1}{z_2},$$

$$\dot{z}_2 = (1 + i\omega_2 - |z_2|^2)z_2 + \varepsilon \frac{1}{z_1} \quad (15)$$

will also preserve rotational symmetry. In terms of real and imaginary parts, this can be written as

$$\dot{x}_i = [1 - (x_i^2 + y_i^2)]x_i - \omega_i y_i + \frac{\varepsilon x_j}{x_j^2 + y_j^2},$$

$$\dot{y}_i = [1 - (x_i^2 + y_i^2)]y_i + \omega_i x_i + \frac{\varepsilon y_j}{x_j^2 + y_j^2}. \quad (16)$$

Shown in Fig. 3 are the three largest LEs for this instance of coupling. The amplitude death region is absent here, and the largest exponent is zero. We find that the exponents are same for co- and counter-rotating oscillators. A phase-locked state is observed in co-rotating oscillators above the coupling value ε_B (indicated in the figure). Here the synchronized frequency is given by $\bar{\omega}$. As counter-rotations are defined to be the oscillators with equal frequency magnitude and opposite directions, this oscillatory dynamics is suppressed for counter-rotating oscillators as $\bar{\omega} = 0$.

A variety of nonlinear functional forms of coupling preserve rotational invariance, such as the coupling terms

$$\frac{P_{n+1}(z_1, z_2)}{P_n(z_1, z_2)} \text{ or } \frac{P_n(z_1^*, z_2^*)}{P_{n+1}(z_1^*, z_2^*)},$$

where P_n is a homogeneous polynomial of degree n . More complex coupling terms that will preserve rotational invariance

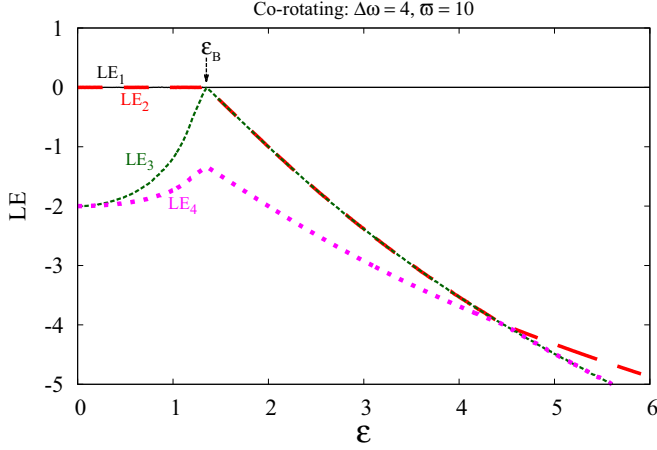


FIG. 3. Lyapunov exponents ($LE_{1,2,3,4}$ are plotted with solid, long-dashed, short-dashed and dotted lines, respectively) of the coupled system for symmetry preserving coupling case [given in Eq. (15)] as a function of ε with $\bar{\omega} = 10$.

can be devised, such as

$$\frac{c_1 z_1 + c_2 z_2}{c_3(z_1 z_2^* + z_2 z_1^*)} \text{ or } \frac{c_3(z_1 z_2^* + z_2 z_1^*)}{c_1 z_1^* + c_2 z_2^*},$$

where c_i are real numbers, and other generalizations that include higher order polynomials in the numerator and denominator.

B. Symmetry-breaking cases

Here we study some simple examples of coupling functions that do not preserve rotational invariance. When two SL oscillators are coupled through a quadratic diffusive-type term, the equations of motion become

$$\begin{aligned} \dot{z}_1 &= (1 + i\omega_1 - |z_1|^2)z_1 + \varepsilon(z_2 - z_1)^2, \\ \dot{z}_2 &= (1 + i\omega_2 - |z_2|^2)z_2 + \varepsilon(z_1 - z_2)^2, \end{aligned} \quad (17)$$

which in terms of real and imaginary parts can be written as

$$\begin{aligned} \dot{x}_i &= [1 - (x_i^2 + y_i^2)]x_i - \omega_i y_i + \varepsilon[(x_j - x_i)^2 - (y_j - y_i)^2], \\ \dot{y}_i &= [1 - (x_i^2 + y_i^2)]y_i + \omega_i x_i + 2\varepsilon(x_j - x_i)(y_j - y_i). \end{aligned} \quad (18)$$

The Jacobian at the fixed point $z^c = (x_1^*, y_1^*, x_2^*, y_2^*) = (0, 0, 0, 0)$ is

$$|J|_{z^c} = \begin{pmatrix} 1 & -\omega_1 & 0 & 0 \\ \omega_1 & 1 & 0 & 0 \\ 0 & 0 & 1 & -\omega_2 \\ 0 & 0 & \omega_2 & 1 \end{pmatrix}, \quad (19)$$

with eigenvalues

$$\lambda_i = 1 \mp i\omega_i. \quad (20)$$

Thus the origin in the coupled system is always unstable.

One can obtain the phase diagram as a function of the parameters ε and $\Delta\omega$ as shown in Fig. 4(a). The labels P and OD correspond to oscillatory and oscillation death regions,

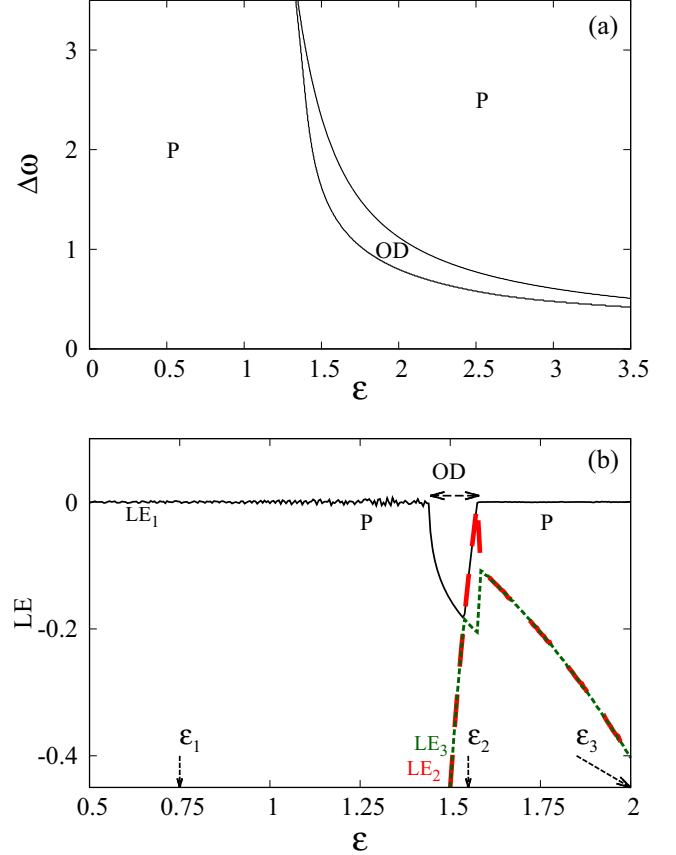


FIG. 4. (a) Different dynamical states observed in the system as a function of ε and $\Delta\omega$ for co-rotating nonlinearly coupled SL oscillators, Eq. (18) (symmetry-breaking case). The dynamics is either periodic (P) or there is oscillation death (OD). (b) Lyapunov exponents (LEs) of the coupled system as a function of coupling strength ε for $\Delta\omega = 2$.

respectively, for co-rotating nonlinear diffusively coupled SL oscillators. The line (enclosing the OD region) indicates the largest LE-changing sign. The details of the different transitions as [indicated in Fig. 4(a)] are depicted in Fig. 4(b) where the LEs of the coupled system Eq. (18) are shown.

Representative trajectories are shown in Fig. 5 with $\omega_1 = 1$ and $\omega_2 = 3$. Initially the motion is periodic as shown in Fig. 5(a) and as ε is increased, the largest LE becomes negative, corresponding to oscillation death. Trajectories leading to the fixed point are shown Fig. 5(b), and on further increasing ε oscillations revive as shown in Fig. 5(c). Note that the periodic motion before OD region is unsynchronized, while subsequent to OD, the periodic motion is phase-synchronized.

There is a significant contrast in the behavior of counter-rotating oscillators. The coupled oscillators show only oscillatory motion, and OD does not occur for this case. The LEs of the coupled system Eq. (18) shown in Fig. 6 for $\Delta\omega = 2$ ($\omega_1 = 1$ and $\omega_2 = -1$) suggests that oscillatory dynamics is revived for counter-rotating oscillators. Details of the trajectories are shown in Fig. 7, where the system is shown to have either incoherent or phase-synchronized oscillatory motion.

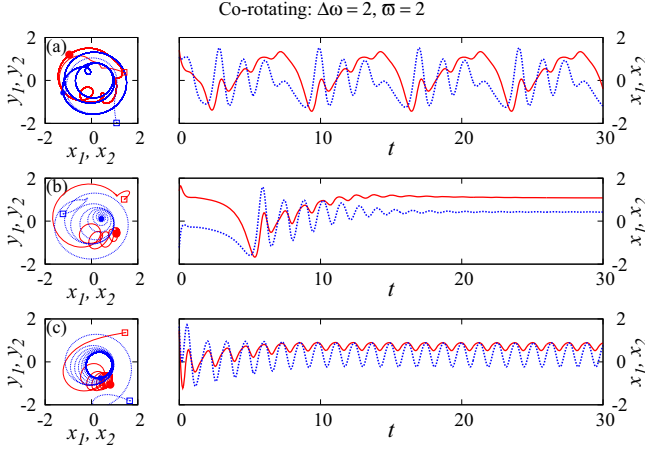


FIG. 5. For nonlinear symmetry-breaking coupling [Eq. (18)] and co-rotating oscillators, shown in the left panel is the behavior of the system in phase space (x_i, y_i plane) at different coupling strengths. Trajectories of two oscillators are shown by solid-red and dotted-blue lines, respectively. The starting point of the two trajectories are shown by open boxes, and the final states are shown by filled circles. The corresponding time series of variables $x_{1,2}$ are plotted in the right panel. Panels (a)–(c), respectively, correspond to the behavior at coupling strength $\varepsilon = 0.75$ (periodic and unsynchronized), 1.55 (oscillation death), and 2.0 (periodic and phase synchronized) as marked in Fig. 4(b).

A second example of symmetry breaking that we consider is the coupling of two SL oscillators as follows:

$$\dot{z}_1 = (1 + i\omega_1 - |z_1|^2)z_1 + \varepsilon(i\bar{z}_2 - z_1), \quad (21)$$

$$\dot{z}_2 = (1 + i\omega_2 - |z_2|^2)z_2 + \varepsilon(i\bar{z}_1 - z_2),$$

which in terms of real and imaginary parts can be written as

$$\begin{aligned} \dot{x}_i &= [1 - (x_i^2 + y_i^2)]x_i - \omega_i y_i + \varepsilon(y_j - x_i), \\ \dot{y}_i &= [1 - (x_i^2 + y_i^2)]y_i + \omega_i x_i + \varepsilon(x_j - y_i). \end{aligned} \quad (22)$$

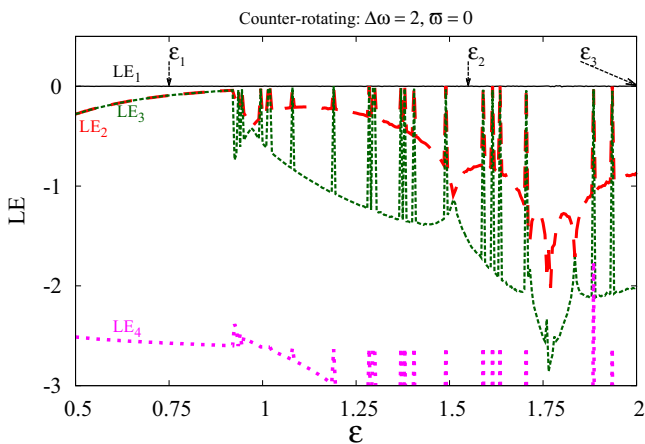


FIG. 6. Lyapunov exponents (LEs) of the system ($LE_{1,2,3,4}$ are plotted with solid, long-dashed, short-dashed, and dotted lines, respectively) as a function of the coupling strength ε for counter-rotating nonlinearly coupled SL oscillators, Eq. (18) (symmetry-breaking case).

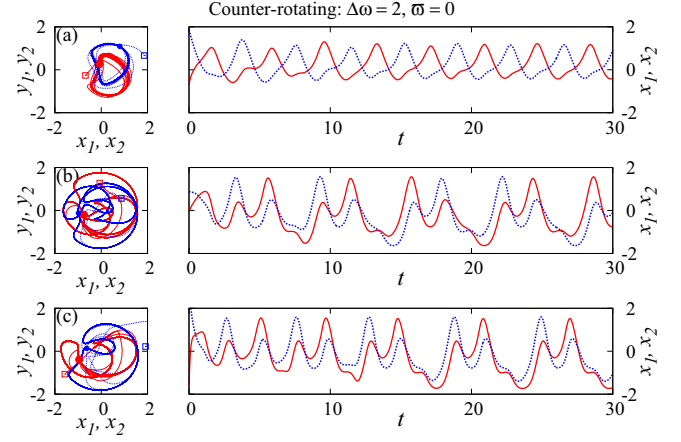


FIG. 7. For nonlinear symmetry-breaking coupling [Eq. (18)] and counter-rotating oscillators, shown in left panel is the behavior of the system in phase space (x_i, y_i plane) at different coupling strength. Trajectories of two oscillators are shown by solid-red and dotted-blue lines, respectively. The starting point of the two trajectories is shown by open boxes, and the final states are shown by filled circles. The corresponding time series of variables $x_{1,2}$ are plotted on the right panel. Panels (a)–(c), respectively, correspond to the periodic behaviors at different coupling strength $\varepsilon = 0.75, 1.55,$ and 2.0 as marked in Fig. 6.

The coupling term thus involves the difference of “dis-similar” variables, which in earlier works has been termed conjugate coupling [14,24–26]. In this case also the origin (denoted z^c) is a trivial fixed point, and the Jacobian matrix is

$$|J|_{z^c=0} = \begin{pmatrix} 1 - \varepsilon & -\omega_1 & 0 & \varepsilon \\ \omega_1 & 1 - \varepsilon & \varepsilon & 0 \\ 0 & \varepsilon & 1 - \varepsilon & -\omega_2 \\ \varepsilon & 0 & \omega_2 & 1 - \varepsilon \end{pmatrix}. \quad (23)$$

The eigenvalues of the Jacobian at the origin in this case are given by

$$\lambda = 1 - \varepsilon \mp \sqrt{\varepsilon^2 - \bar{\omega}^2} \mp i \frac{\Delta\omega}{2}, \quad (24)$$

the real and imaginary parts being

$$\begin{aligned} \text{Re}(\lambda) &= (1 - \varepsilon), \text{ if } \varepsilon \leq \bar{\omega} \\ &= (1 - \varepsilon) \mp \sqrt{\varepsilon^2 - \bar{\omega}^2}, \text{ if } \varepsilon > \bar{\omega} \end{aligned} \quad (25)$$

and

$$\begin{aligned} \text{Im}(\lambda) &= \mp \sqrt{|\varepsilon^2 - \bar{\omega}^2|} \mp \frac{\Delta\omega}{2}, \text{ if } \varepsilon \leq \bar{\omega}, \\ &= \mp \frac{\Delta\omega}{2}, \text{ if } \varepsilon > \bar{\omega}. \end{aligned} \quad (26)$$

In contrast to the earlier case of coupling through similar variables, in the conjugate coupling case the real part of the eigenvalues and hence the stability of the fixed point is affected by the case of counter-rotating oscillators. Since $\bar{\omega} = 0$, $\text{Re}(\lambda) = 1$, and thus the fixed point at the origin is *never* stable. For co-rotating oscillators (both identical or mismatched) the origin stays stable between the critical coupling values $\varepsilon_A = 1$ and $\varepsilon_B = \frac{1}{2}(1 + \bar{\omega}^2)$ [Fig. 8(a)].

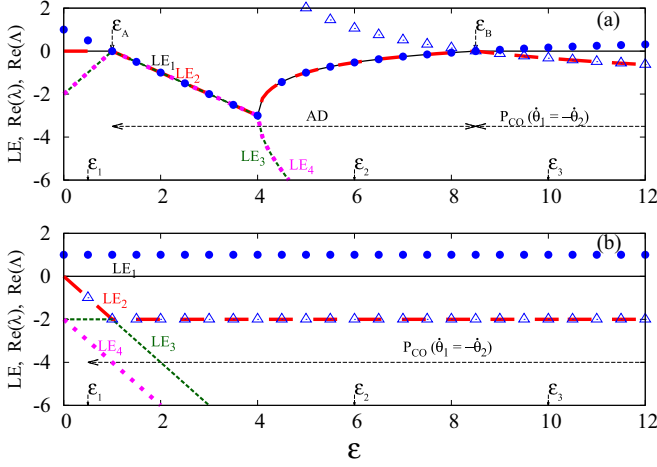


FIG. 8. Lyapunov exponents (LEs) for conjugate coupling through dissimilar variables [Eq. (22)] ($LE_{1,2,3,4}$ are plotted with solid, long-dashed, short-dashed, and dotted lines, respectively) as a function of coupling strength ε , along with the real part of the eigenvalues of the Jacobian λ [filled circle, Eq. (25)], Λ [open triangles, Eq. (31)] for (a) mismatched co-rotating $\Delta\omega = 4$, $\bar{\omega} = 4$ and (b) counter-rotating $\Delta\omega = 4$, $\bar{\omega} = 0$ oscillators.

The equations for amplitudes and phases in polar coordinates now become

$$\begin{aligned} \dot{r}_i &= r_i(1 - \varepsilon - r_i^2) + \varepsilon r_j \sin(\theta_i + \theta_j), \\ \dot{\theta}_i &= \omega_i + \varepsilon \frac{r_j}{r_i} \cos(\theta_i + \theta_j), \quad i, j = 1, 2, \quad i \neq j. \end{aligned} \quad (27)$$

In the variable $\theta = (\theta_1 + \theta_2)$ symmetric solutions with $r_1 = r_2$ are given by the equation of motion

$$\begin{aligned} \dot{r} &= r(1 - \varepsilon - r^2) + \varepsilon r \sin \theta, \\ \dot{\theta} &= 2\bar{\omega} + 2\varepsilon \cos \theta, \end{aligned} \quad (28)$$

with the steady-state solution

$$\begin{aligned} r^{*2} &= 1 - \varepsilon \pm \sqrt{\varepsilon^2 - \bar{\omega}^2}, \\ \theta^* &= \arccos(-\bar{\omega}/\varepsilon). \end{aligned} \quad (29)$$

Thus stationary solutions exist for $\varepsilon \geq \bar{\omega}$, with the frequencies of the individual oscillators given by $\dot{\theta}_1 = -\Delta\omega/2$ and $\dot{\theta}_2 = +\Delta\omega/2$.

When the co-rotating oscillators are mismatched, $\Delta\omega \neq 0$, this represents a dynamics with equal amplitudes r^* and counter-oscillations (denoted P_{CO} [27]) in individual oscillators ($\dot{\theta}_1 = -\dot{\theta}_2$) and corresponds to mixed synchronization [17,27]. The stability of such solutions [Eq. (29)] can be estimated as before from the corresponding Jacobian

$$\mathbf{H} = \begin{pmatrix} 1 - \varepsilon - 3r^{*2} + \varepsilon \sin \theta^* & -\varepsilon r^* \cos \theta^* \\ 0 & -2\varepsilon \sin \theta^* \end{pmatrix}, \quad (30)$$

the eigenvalues of which are

$$\begin{aligned} \Lambda_1 &= -2(1 - \varepsilon) \mp 2\sqrt{\varepsilon^2 - \bar{\omega}^2}, \\ \Lambda_2 &= \mp 2\sqrt{\varepsilon^2 - \bar{\omega}^2}. \end{aligned} \quad (31)$$

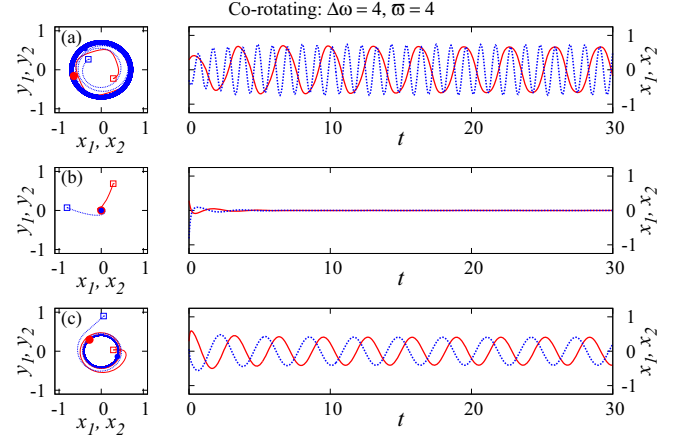


FIG. 9. Trajectories in the phase space (left panel) and corresponding time series of variable $x_{1,2}$ (right panel) are plotted at different coupling values (a) $\varepsilon = 0.5$, (b) $\varepsilon = 6$, and (c) $\varepsilon = 10$ for conjugate coupling and mismatched co-rotating oscillators system $\Delta\omega = 4$, $\bar{\omega} = 4$. Trajectories of two oscillators are shown by solid-red and dotted-blue lines, respectively. The starting point of the two trajectories is shown by open boxes, and the final states are shown by filled circles.

The stability condition for these solutions is given by

$$\varepsilon > \frac{1}{2}(1 + \bar{\omega}^2). \quad (32)$$

Note that for co-rotating oscillators the critical value of the coupling where these solutions [Eq. (29)] become stable is the point where origin loses its stability.

In the numerical simulations below, for the co-rotating oscillators we have taken $\bar{\omega} = 4$ and $\Delta\omega = 4$, and for counter-rotating oscillators we consider $\bar{\omega} = 0$ with $\Delta\omega = 4$, respectively. The LEs of the system [Eq. (22)] and real part of the eigenvalues, Eq. (25) and (31) are shown in Fig. 8 for the two cases of (1) co-rotating oscillators and (2) counter-rotating oscillators.

In the co-rotating case the origin is stable between $\varepsilon_A = 1$ and $\varepsilon_B = \frac{1}{2}(1 + \bar{\omega}^2) = 8.5$ since in this region, $\text{Re}(\lambda)$ [shown by blue circles in Fig. 8(a)] is negative. For counter-rotations [Fig. 2(b)], the origin remains unstable for the whole range since $\text{Re}(\lambda) = 1$. Furthermore the solutions described in Eq. (29) stabilize at $\varepsilon = \frac{1}{2}(1 + \bar{\omega}^2) = 8.5$ (for co-rotations) and $\varepsilon = 0.5$ (for counter-rotations), when $\text{Re}(\Lambda)$ (shown by triangles) crosses zero and becomes negative. These solutions correspond to the dynamics with equal amplitudes but frequencies of opposite signs, namely, counter-oscillations (P_{CO}): $\dot{\theta}_1 = -\dot{\theta}_2$ in both cases (a) and (b). Trajectories in phase space and time series for one of the variables are shown in Fig. 9 (co-rotating with mismatched frequencies) and Fig. 10 (counter-rotating oscillators) at selected values of ε that are marked in Fig. 8.

Therefore, whenever SL oscillators are coupled so as to break rotational symmetry, co- and counter-rotating oscillators will have contrasting dynamical behavior.

III. SUMMARY

Our interest in the present work has been in analyzing the dynamical consequences of symmetry breaking in coupled

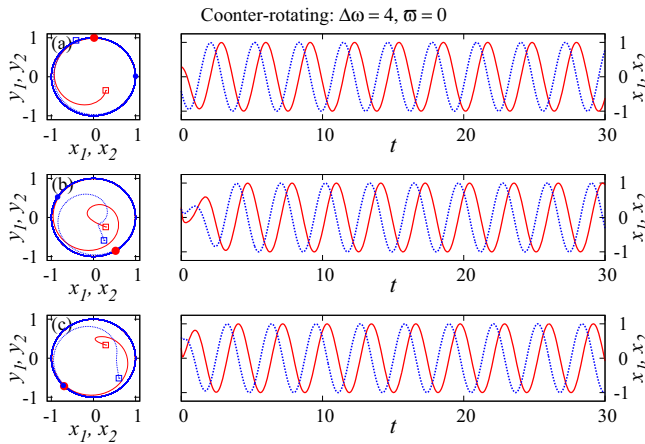


FIG. 10. Trajectories in the phase space (left panel), and corresponding time series of variable $x_{1,2}$ (right panel) are plotted at different coupling values (a) $\varepsilon = 0.5$ and (b) $\varepsilon = 6$ for conjugate coupling in counter-rotating system $\Delta\omega = 4, \bar{\omega} = 0$. Trajectories of two oscillators are shown by solid-red and dotted-blue lines, respectively. The starting point of the two trajectories is shown by open boxes, and the final states are shown by filled circles.

oscillator systems with co- and counter-rotations. We have examined here the example of coupled Stuart-Landau oscillators: these have continuous symmetry, the equation of motion being invariant under a rotational transformation.

When coupled, the rotational invariance can be preserved or broken, and here we show that there are subtle effects that depend on the details of the coupled oscillators. In particular, oscillators with phase velocities that have opposite sign, namely, counter-rotating oscillators behave differently from the case when the velocities have the same sign (co-rotation).

A well-known phenomenon that occurs in coupled SL (and other) oscillator systems is that of oscillation death, when the coupled oscillators drive each other to a situation when neither oscillates. This occurs when the coupling stabilizes an otherwise unstable fixed point, or the coupling creates a new stable fixed point. In counter-rotating systems when the symmetry is broken, the regime of oscillation death is suppressed.

We believe that the present results have wide applicability. The SL system is representative of the generic behavior near a Hopf bifurcation, and therefore this is a good model for a typical nonlinear oscillator. The SL system is related not only to the Ginzburg-Landau equation but also describes the general two-dimensional solution of the Navier-Stokes equations [28,29], and thus this model applies to wide variety of situations. In addition, the sign of the phase velocity can be of relevance in several instances such as cyclic flows in plasma [30], atmospheric and oceanic currents [31], and biological media [32]. In such cases the interaction of units with oscillations in the same or opposite directions can be of relevance [33–35]. Motion in opposing directions can significantly modify the resulting behavior, particularly affecting the nature of synchronization [17,36] and oscillation quenching. This needs special consideration in the context of designing control strategies in order to lead the system to a specific desired state using various internal or external parameters.

Apart from oscillation quenching, counter-rotations may also effect the nature of synchronization giving rise to a new type of “mixed synchronization” [17], where one can observe positive and negative correlations simultaneously in different variables of the system. Recent studies have drawn attention to the significance of including sense of directions in the motion and its possible effects on the dynamics [17,36–39]. However, further investigation is required to analyze the combined effects of counter-rotations in the systems with symmetry-breaking coupling, especially when other factors are also considered such as time delay or dimensionality. These and similar questions are being addressed in our ongoing work [40].

ACKNOWLEDGMENTS

R.R. acknowledges the Department of Science and Technology (DST, India) for support through the J. C. Bose National Fellowship. A.P., V.V., and N.P. thank the Department of Science and Technology as well for research support. N.P. also acknowledges the Max Planck Society, Germany, for support.

- [1] S. H. Strogatz, *Nonlinear Dynamics and Chaos, with Applications to Physics, Biology, Chemistry, and Engineering* (Perseus Books, New York, 1994).
- [2] A. Pikovsky, M. Rosenblum, and J. Kurths, *Synchronization: A Universal Concept in Nonlinear Science* (Cambridge University Press, Cambridge, 2001).
- [3] Y. Kuramoto, *Chemical Oscillations, Waves and Turbulence* (Springer-Verlag, Berlin, 1984).
- [4] A. T. Winfree, *J. Theor. Biol.* **16**, 15 (1967); S. H. Strogatz, *Sync: The Emerging Science of Spontaneous Order* (Hyperion Press, New York, 2003); K. Bar-Eli, *J. Phys. Chem.* **88**, 6174 (1984).
- [5] T. Stankovski, T. Pereira, P. V. McClintock, and A. Stefanovska, *Rev. Mod. Phys.* **89**, 045001 (2017).
- [6] M. G. Rosenblum, A. S. Pikovsky, and J. Kurths, *Phys. Rev. Lett.* **78**, 4193 (1997).
- [7] H. Daido, *Phys. Rev. Lett.* **68**, 1073 (1992); *Prog. Theor. Phys.* **77**, 622 (1987); Y. Chen, J. Xiao, W. Liu, L. Li, and Y. Yang, *Phys. Rev. E* **80**, 046206 (2009); H. Hong and S. H. Strogatz, *ibid.* **84**, 046202 (2011); B. Ottino-Löffler and S. H. Strogatz, *Phys. Rev. Lett.* **120**, 264102 (2018).
- [8] S. Watanabe and S. H. Strogatz, *Phys. Rev. Lett.* **70**, 2391 (1993); *Physica D (Amsterdam)* **74**, 197 (1994).
- [9] M. J. Panaggio and D. M. Abrams, *Nonlinearity* **28**, R67 (2015).
- [10] K. Bar-Eli, *Physica D (Amsterdam)* **14**, 242 (1985); R. E. Mirollo and S. H. Strogatz, *J. Stat. Phys.* **60**, 245 (1990); G. B. Ermentrout, *Physica D (Amsterdam)* **41**, 219 (1990).

- [11] D. G. Aronson, G. B. Ermentrout, and N. Kopell, *Physica D (Amsterdam)* **41**, 403 (1990).
- [12] D. V. Ramana Reddy, A. Sen, and G. L. Johnston, *Phys. Rev. Lett.* **80**, 5109 (1998).
- [13] F. M. Atay, *Phys. Rev. Lett.* **91**, 094101 (2003).
- [14] R. Karnatak, R. Ramaswamy, and A. Prasad, *Phys. Rev. E* **76**, 035201 (2007).
- [15] G. Saxena, A. Prasad, and R. Ramaswamy, *Phys. Rep.* **521**, 205 (2012); G. Saxena, N. Punetha, A. Prasad, and R. Ramaswamy, *AIP Conf. Proc.* **1582**, 158 (2014); A. Koseska, E. Volkov, and J. Kurths, *Phys. Rep.* **531**, 173 (2013); A. Prasad, *Phys. Rev. E* **72**, 056204 (2005).
- [16] V. Garcia-Morales and K. Krischer, *Contemp. Phys.* **53**, 79 (2012).
- [17] A. Prasad, *Chaos Solitons Fractals* **43**, 42 (2010).
- [18] K. Premalatha, V. K. Chandrasekar, M. Senthilvelan, and M. Lakshmanan, *Phys. Rev. E* **91**, 052915 (2015).
- [19] I. Schneider, M. Kapeller, S. Loos, A. Zakharova, B. Fiedler, and E. Schöll, *Phys. Rev. E* **92**, 052915 (2015).
- [20] A. Zakharova, M. Kapeller, and E. Schöll, *J. Phys. (Conf. Ser.)* **727**, 012018 (2016).
- [21] G. C. Sethia, A. Sen, and F. M. Atay, *Phys. Rev. Lett.* **100**, 144102 (2008).
- [22] A. Gjurchinovski, A. Zakharova, and E. Schöll, *Phys. Rev. E* **89**, 032915 (2014).
- [23] K. Sathiyadevi, S. Karthiga, V. K. Chandrasekar, D. V. Senthikumar, and M. Lakshmanan, *Phys. Rev. E* **95**, 042301 (2017).
- [24] M. Y. Kim, R. Roy, J. L. Aron, T. W. Carr, and I. B. Schwartz, *Phys. Rev. Lett.* **94**, 088101 (2005).
- [25] G. Goleniewski, *Biom. J.* **38**, 281 (1996); R. Karnatak, R. Ramaswamy, and U. Feudel, *Chaos Solitons Fractals* **68**, 48 (2014).
- [26] T. Ueta and H. Kawakami, Chaos in cross-coupled BVP oscillators, *Proceedings of the International Symposium on Circuits and Systems (ISCAS '03)*, 25–28 May 2003, Bangkok, Thailand (IEEE, 2003), Vol. 3, p. III; T. Singla, N. Pawar, and P. Parmananda, *Phys. Rev. E* **83**, 026210 (2011).
- [27] P_{CO} refers to the case when oscillators move in opposite direction: these stationary-state solutions [Eq. (29)] require that the frequencies $\dot{\theta}_1(t) = -\dot{\theta}_2(t) = |\Delta\omega/2|$. Also, due to the constraint in the dynamics [Eq. (29)], different variables of one system have different correlations with those of another oscillator. Such emergence of *mixed* correlations in different variables is referred to as mixed synchronization [17].
- [28] J. Stuart, *J. Fluid Mech.* **9**, 353 (1960).
- [29] M. Provansal, C. Mathis, and L. Boyer, *J. Fluid Mech.* **182**, 1 (1987); P. Le Gal, A. Nadim, and M. Thompson, *J. Fluid Struct.* **15**, 445 (2001).
- [30] G. N. Throumoulopoulos and H. Tasso, *Phys. Plasmas* **17**, 032508 (2010).
- [31] H. Fukuta and Y. Murakami, *Phys. Rev. E* **57**, 449 (1998); Y. Murakami and H. Fukuta, *Fluid Dyn. Res.* **31**, 1 (2002); P. Meunier and T. Leweke, *J. Fluid Mech.* **533**, 125 (2005).
- [32] S. Takagi and T. Ueda, *Physica D (Amsterdam)* **237**, 420 (2008).
- [33] S. Thanvanthri, K. T. Kapale, and J. P. Dowling, *Phys. Rev. A* **77**, 053825 (2008); K. T. Kapale and J. P. Dowling, *Phys. Rev. Lett.* **95**, 173601 (2005).
- [34] P. Billant, P. Brancher, and J.-M. Chomaz, *Phys. Fluid* **11**, 2069 (1999).
- [35] J. M. Newby and M. A. Schwemmer, *Phys. Rev. Lett.* **112**, 114101 (2014).
- [36] S. K. Bhowmick, D. Ghosh, and S. K. Dana, *Chaos* **21**, 033118 (2011).
- [37] V. Varshney, G. Saxena, B. Biswal, and A. Prasad, *Chaos* **27**, 093104 (2017).
- [38] A. Mari, A. Farace, N. Didier, V. Giovannetti, and R. Fazio, *Phys. Rev. Lett.* **111**, 103605 (2013).
- [39] M. A. Schwemmer and J. M. Newby, *Physica D (Amsterdam)* **317**, 15 (2016).
- [40] N. Punetha (unpublished).